Spectrochimica Acta Part B 101 (2014) 220–225

Contents lists available at ScienceDirect

Spectrochimica Acta Part B

journal homepage: www.elsevier.com/locate/sab

Analytical Note

Identification of quantum dots labeled metallothionein by fast scanning laser-induced breakdown spectroscopy ☆

Marie Konecna [a,b], Karel Novotny [c], Sona Krizkova [a,b], Iva Blazkova [b], Pavel Kopel [a,b], Jozef Kaiser [a,d], Petr Hodek [e], Rene Kizek [a,b], Vojtech Adam [a,b,*]

[a] Central European Institute of Technology, Brno University of Technology, Technicka 3058/10, CZ-616 00 Brno, Czech Republic
[b] Department of Chemistry and Biochemistry, Faculty of Agronomy, Mendel University in Brno, Zemedelska 1, CZ-613 00 Brno, Czech Republic
[c] Central European Institute of Technology, Masaryk University, Kamenice 753/5, CZ-625 00 Brno, Czech Republic
[d] Institute of Physical Engineering, Brno University of Technology, Technicka 2, CZ-616 69 Brno, Czech Republic
[e] Department of Biochemistry, Faculty of Science, Charles University in Prague, Hlavova 2030/8, CZ-128 00 Prague,Czech Republic

ARTICLE INFO

Article history:
Received 31 December 2013
Accepted 21 August 2014
Available online 30 August 2014

Keywords:
Laser-induced breakdown spectroscopy
Cadmium
Quantum dot
Metallothionein
Immunoassay

ABSTRACT

The technique described in this paper allows detection of quantum dots (QDs) specifically deposited on the polystyrene surface by laser-induced breakdown spectroscopy (LIBS). Using LIBS, the distribution of QDs or their conjugates with biomolecules deposited on the surface can be observed, regardless of the fact if they exhibit fluorescence or not. QDs deposited on the specific surface of polystyrene microplate in the form of spots are detected by determination of the metal included in the QDs structure. Cd-containing QDs (CdS, CdTe) stabilized with mercaptopropionic (MPA) or mercaptosuccinic (MSA) acid, respectively, alone or in the form of conjugates with metallothionein (MT) biomolecule are determined by using the 508.58 nm Cd emission line. The observed absolute detection limit for Cd in CdTe QDs conjugates with MT in one spot was 3 ng Cd. Due to the high sensitivity of this technique, the immunoanalysis in combination with LIBS was also investigated. Cd spatial distribution in sandwich immunoassay was detected.

1. Introduction

Determination of metallothionein (MT) has become important due to its potential role as a tumor disease marker [1–3]. The most of biological functions suggested for MT is related to its metal-binding and antioxidant function [2]. For MT determination enzyme-linked immunosorbent assay (ELISA) can be advantageously used [4,5]. The most frequently used labels are enzymes or fluorescent molecules or nanoparticles with absorbance or fluorescence detection [6–8]. However, the results of optical measurements can be affected by optical properties of the samples or solutions, or by the fluorescence or matrix interference. Another issue is the linear range of the assay and the low stability of the signal. Better results can be obtained by non-optical methods including electrochemistry, where electrochemical activity of the product of enzymatic activity is measured [9–13].

All the above mentioned assays highly demand on robust laboratory equipment, which is hardly to be used in situ. Different strategies leading to miniaturization, automation, microfluidics and portable devices development are, therefore, investigated [14,15]. From this reason a non-optical dry and automated method of immunoassay evaluation is beneficial. An example of such application is a postponed evaluation of immunoassay results after long-term remote samples collecting. One possibility of the sample storage is injection of the liquid sample (i.e. blood) on the specific surface, especially filtration paper in the form of dried spots and later analyzed [16–18].

The wide range of various applications and types of samples has been already analyzed by laser-induced breakdown spectroscopy (LIBS) [19–21]. One of the fastest evolving fields of LIBS application is the analysis of bio-samples as it was described by Kaiser et al. [22], where selected biological LIBS applications including cells, microorganisms, animal tissues, plant samples or biominerals are overviewed. The main advantage of the LIBS method is the possibility of investigation of the elemental spatial distribution. Kidney slices from a mouse were analyzed by LIBS after injection of a solution of gadolinium-based nanoparticles [23]. The presented procedure of quantifying Gd in the tissue by LIBS was in good agreement with measurement performed by ICP-OES. Determination of nanoparticles by LIBS was described on the example of two metaloxide nanoparticles, titanium dioxide (TiO_2) and a rare earth sesquioxide nanoparticle, holmium oxide (Ho_2O_3) [24]. Nanoparticles in aqueous solution are identified and quantified by complementary LIBS and Raman spectroscopy. This approach can be applied to fully characterize the nanoparticle elemental composition

☆ Selected paper from the 7th Euro-Mediterranean Symposium on Laser Induced Breakdown Spectroscopy (EMSLIBS 2013), Bari, Italy, 16–20 September 2013.

* Corresponding author at: Department of Chemistry and Biochemistry, Mendel University in Brno, Zemedelska 1, CZ-613 00 Brno, Czech Republic, European Union. Tel.: +420 5 4513 3350; fax: +420 5 4521 2044.
E-mail address: vojtech.adam@mendelu.cz (V. Adam).

http://dx.doi.org/10.1016/j.sab.2014.08.037
0584-8547/

in aqueous environments and to determine their size with a detection limit of a few nanometers. In addition, gold on ferromagnetic nanoparticles was analyzed and quantified by LIBS method after the fixation of powdered samples in the form of UV hardened gel [25]. The new approach in nanoparticle utilization is their deposition on the surface of the metallic sample which results in Nanoparticle-Enhanced LIBS. In the presence of silver nanoparticles an increase of 1–2 orders of magnitude in LIBS signals was obtained [26]. In our previous study porous carrier materials were studied in terms of CdS and CdTe QDs detection by double pulse LIBS after injection of small volumes of QDs solutions [27].

In this study the combination of LIBS with immunoanalysis procedures is described. The detection of biomolecules is based on the labeling with Cd-containing quantum dots. Cadmium spatial distribution is determined using its emission line at 508.58 nm. In the first part quantum dots or their conjugates with metallothionein are injected on the polystyrene surface of the reverse side of microtitration plate and the basic analytical characteristics of LIBS measurements are defined. The distribution of QDs on the surface is also observed by fluorescence measurement as a comparative technique. The total amount of Cd in prepared solutions is determined by atomic absorption spectrometry. In the second part of our work the antibody sandwich immunoassay is prepared and LIBS map of Cd spatial distribution is measured.

2. Materials and methods

2.1. Chemicals

All chemicals were purchased from Sigma-Aldrich (USA). Deionized water underwent demineralization by reverse osmosis using an apparatus Aqua Osmotic 02 (Aqua Osmotic, Tisnov, Czech Republic) and was subsequently purified using a Millipore RG (MilliQ, USA). Deionized water was used for preparation of all solutions.

2.2. Preparation of stock solution of QDs

QDs containing CdS stabilized with mercaptopropionic acid (MPA) were prepared using a slightly modified method published in Ref. [28]. Briefly, cadmium nitrate tetrahydrate $Cd(NO_3)_2 \cdot 4H_2O$ was dissolved in ACS water (25 ml). 3-mercaptopropionic acid (35 μl, 0.4 mmol l^{-1}) was slowly added to the stirred solution. Afterwards, pH was adjusted to 9.1 with 1 mol l^{-1} NH_3 (1.5 ml). Sodium sulfide nanohydrate $Na_2S \cdot 9H_2O$ (0.1 mmol l^{-1}) in 23 ml of ACS water was poured into the first solution under vigorous stirring. Obtained yellow solution was stirred for 1 h. CdS QDs were stored in dark at 4 °C.

Spare solution of CdTe QDs was prepared by dissolving cadmium acetate dihydrate $Cd(CH_3COO)_2 \cdot 2H_2O$ in 76 ml of Milli-Q water in a 200 ml beaker on a magnetic stirrer. Mercaptosuccinic acid (MSA) (60 mg) in water (1 ml) was added followed by 1.8 ml of 1 mol l^{-1} NH_3. Finally, a solution of Na_2TeO_3 (0.0055 g) in water was added and after few minutes 40 mg of $NaBH_4$ was poured to the stirred solution. The solution was stirred for 1 h, volume was adjusted to 100 ml with addition of water and after that it was heated in vials filled with 2 ml of the solution in microwave oven Multiwave 300 (Anton Paar, Austria) (300 W, 120 °C, 10 min).

Streptavidin QDs were prepared by mixing 2 ml CdTe QDs with 28 μl of streptavidin (5 mg/ml) and shaking on orbital shaker Multi RS-60 (Biosan, Latvia) for 12 h at 500 RPM.

2.3. Metallothionein isolation and preparation of MT and QDs solution

MT was isolated from rabbit liver as described in Ref. [9]. Sets of various concentration of MT (0–23 μmol l^{-1}) solution were mixed with various concentrations of CdS QDs or CdTe QDs (0–200 ng μl^{-1}) solution and left to interact for 24 h with constant shaking [29].

2.4. Preparation of the spots on the polystyrene surface

5 μl of each prepared sample (QDs, QDs and MT) was pipetted into 10 μl of 50 mmol l^{-1} carbonate buffer (32 mmol l^{-1} Na_2CO_3 and 68 mmol l^{-1} $NaHCO_3$, pH 9.6) on a reverse side of standard 96-well polystyrene microplate (Thermo Fisher Scientific, USA) and dried using Ultravap 96 Blowdown Evaporator (Porvair Sciences, Ltd., United Kingdom) under nitrogen atmosphere.

2.5. Sandwich immunoassay

In order to perform the laser ablation, the immunoassay was processed on a reverse side of standard 96-well polystyrene microtitration plate. The preparation of antibodies and optimization of the immunoassay is described in Refs. [4,30]. The volume of 20 μl of the antibodies diluted 1:3000 (*v*/*v*) in 50 mmol l^{-1} carbonate buffer was adsorbed on polystyrene surface for 1 h at 37 °C. During the adsorption and all incubation steps the plate was covered to prevent evaporation of the liquid. Free surface of the microplate was blocked with 20 μl of 1% bovine serum albumin (BSA) in phosphate buffered saline (PBS, 137 mmol l^{-1} NaCl, 2.7 mmol l^{-1} KCl, 1.4 mmol l^{-1} NaH_2PO_4, and 4.3 mmol l^{-1} Na_2HPO_4, pH 7.4) for 30 min at 37 °C. PBS was also used for washing the wells and as a diluent in following steps. After washing the wells for 2× with 20 μl of PBS for 5 min, 10 μl of MT sample was added and the plate was incubated for 1 h at 37 °C. After the incubation and washing (see above), 20 μl of the biotinylated antibodies diluted 1:200 was added and the plate was incubated for 1 h at 37 °C. Then the plate was washed and 20 μl of streptavidin-conjugated QDs was added and the plate was incubated for 30 min at 37 °C. After washing and drying using the Ultravap 96 Blowdown Evaporator (Porvair Sciences, Ltd., United Kingdom) the LIBS and fluorescence measurements were performed in triplicates.

2.6. LIBS instrumentation

The modified laser system UP-266 MACRO equipped with software-controlled movement in *x* and *y* directions was used (Fig. 1A). The prepared microplate with injected spots was placed into a lab-made holder (Fig. 1B). Pulse energy was set to 10 mJ while plasma emission was collected and transported by means of a 3 m long optical fiber into the entrance of a monochromator (Jobin Yvon, TRIAX 320) and detected with the ICCD detector (Princeton, PI MAX 3). The delay of the signal detection after laser pulse was 0.5 μs and the integration time was 5 μs. The raster covered 15 × 15 points with spacing 500 μm while laser spot diameter was approximately 100 μm (Fig. 1C and D). The intensity of Cd (I) 508.58 nm emission line was measured and the resulting values were evaluated from maximum line intensity after appropriate background subtraction. No further intensity normalization or correction was used. These data allowed the construction of 2D maps showing the spatial distribution of Cd (i.e. QDs) in the spot.

2.7. Fluorescence measurement

Monitoring of fluorescence was performed using an In Vivo Xtreme system by Carestream (Rochester, NY, USA) equipped with a 400 W xenon light source and 28 excitation filters (410–760 nm) and a 4MP CCD camera. The excitation and emission wavelengths were set in accordance with absorption and fluorescence spectra measured for each type of QDs.

2.8. Measurement of cadmium by atomic absorption spectrometry

Measurements were carried out on a 240 FS AA Agilent Technologies atomic absorption spectrometer with a deuterium lamp background correction. Cadmium hollow cathode lamp (Agilent, USA) was used as a source of radiation. The spectrometer was operated at the 228.8 nm

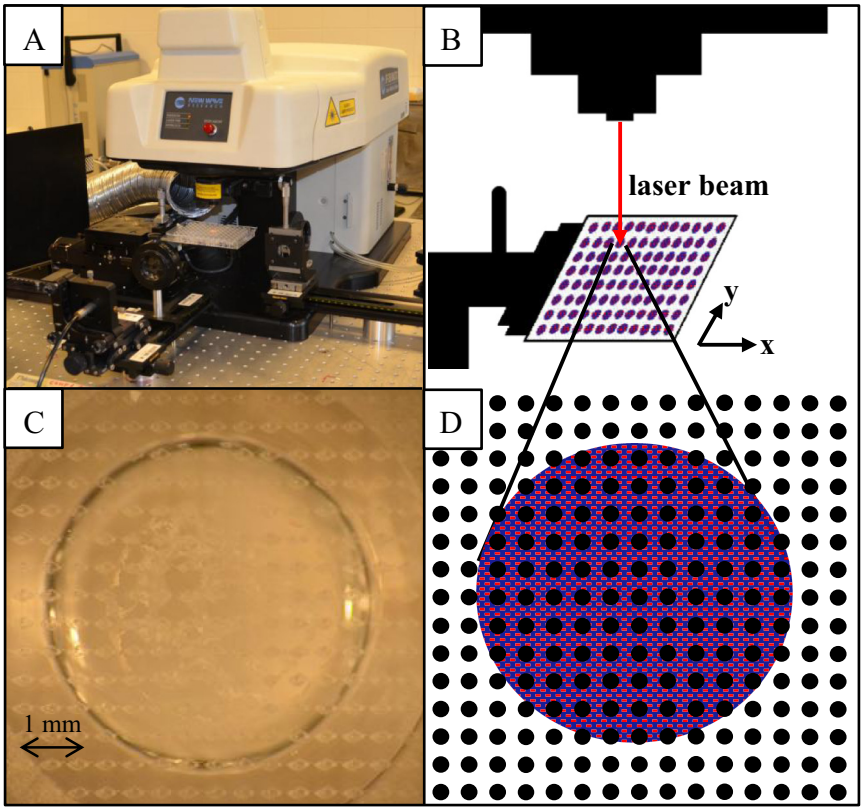

Fig. 1. (A) The image of reverse side of polystyrene microtitration desk placed in UP-266 MACRO device for LIBS. (B) The scheme of the location of the microplate with spots in lab-made holder allowing programmed shifts in the *x* and *y* directions and the direction of laser beam. (C) The image of one spot after laser ablation where the craters can be seen. (D) The schematic raster grid with spot position.

resonance line with a lamp current of 4 mA and a spectral bandwidth of 0.5 nm. The flame type air-acetylene was used.

3. Results and discussion

Cadmium containing spots deposited on polystyrene microplate surface was measured by LIBS in raster mode (Fig. 1C and D). Both types of QDs, CdS and CdTe or in the mixture with MT were investigated. Before deposition of the solutions on the polystyrene surface all of them were analyzed by AAS and Cd was determined to verify Cd concentration. The amount of Cd in each spot in accordance with injected 5 μl of sample volume was 1 μg, or 0.5 μg in the mixture with MT. The comparison of LIBS and fluorescence measurement is shown in Fig. 2. While the fluorescence signal is connected directly to the QDs distribution the LIBS signal corresponding to distribution of Cd. Although fluorescence maps are characterized by better spatial resolution than LIBS maps, the obtained

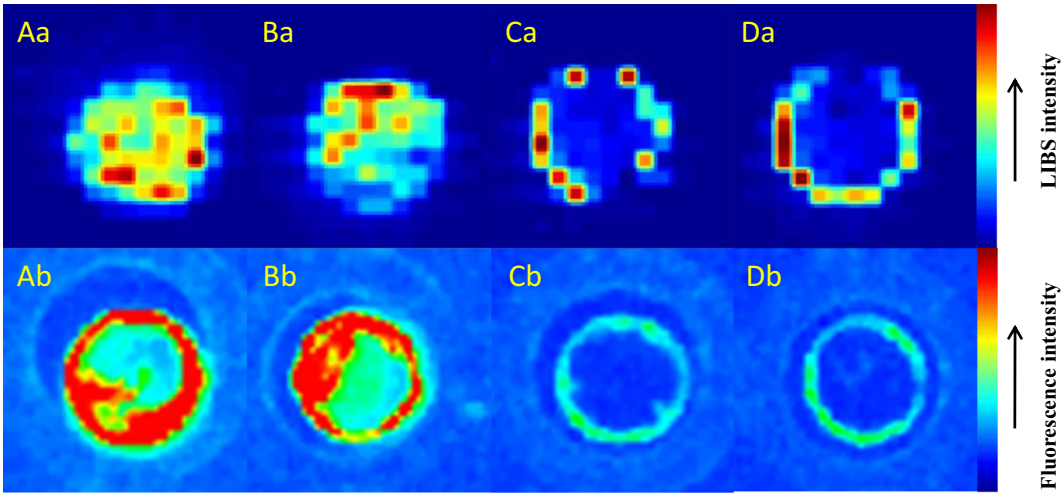

Fig. 2. Comparison of LIBS Cd maps (top line) and fluorescence images (bottom line) of four different types of spots: (A) CdS QDs and (B) QDs CdTe and their mixtures with metallothionein (C) CdS QDs-MT or (D) CdTe QDs-MT. In the absence of biomolecules the Cd is noticeable over the whole area but the spreading is not regular. In the presence of biomolecules the effect of drying appears. Injected volume of the samples was 5 μl, the amount of Cd 1000 ng, in the presence of MT the amount of Cd was 500 ng, the amount of MT was 17 pg in the spot. Images were obtained by LIBS (raster 15 × 15 points with spacing 500 μm, diameter of laser spot was approximately 100 μm, intensity on emission line Cd (I) 508.58 nm) and fluorescence (excitation wavelength 460 nm, emission wavelength 700 nm).

results of distribution are comparable. On the other hand, LIBS emission intensity showed higher signal to noise ratio. Distributions of CdS and CdTe QDs measured by LIBS are shown in Fig. 2Aa and Ba, respectively. Distributions of complexes of these QDs with MT within a spots are in Fig. 2Ca and Da respectively. Fig. 2Ab–Db demonstrates corresponding distribution maps obtained by fluorescence measurements. There is no difference between each type of QDs (CdS, CdTe) in terms of their spread on the surface after drying. Both types of QDs deposited in the form of water solution in the absence of biomolecule the signal of Cd occurs over the whole surface of the spot. The maps show Cd over the whole area of the spot but the spreading is irregular. Poor tacking of particles on the polystyrene surface and easy falling off of the sample was also observed in the absence of biomolecule. As an expression of this fact, high relative standard deviation (RSD) of the measurements was found. In the case of spots containing QDs and MT the effect of drying appears for both types of QDs (CdS, CdTe). The fluorescence signal corresponds to the LIBS measurement. Based on the results obtained we decided to use CdTe QDs for further experiments, because they provided slightly higher fluorescence signal.

3.1. The influence of polystyrene surface

Pulsed radiation at a wavelength of 266 nm generates a micro-plasma characterized by various atomic and molecular transitions that can be directly applied for LIBS based detection. While the elemental analysis of atomic transitions is clearly defined and recorded in different databases (National Institute of Standards and Technology (NIST)), the interference effects of molecular transitions negatively affecting analyte signal are still under investigation. The most frequently studied are transitions of diatomic molecules of interest that include diatomic CN, C_2, CO. Polystyrene is also a source of background noise caused by organic polymer compounds (Fig. 3). In accordance with Pearse [31], the bands, which appeared, are of very frequent occurrence in sources containing carbon and deal with C_2 bands. One of the main head lies in our spectral window around the wavelength of 512 nm and also around 509 nm. The structured background of the polystyrene appeared only outside the spot while during ablation of the spot area this background was diminished.

3.2. The effect of different Cd-QDs and MT concentration

Sets of different concentration of CdTe QDs were injected on the polystyrene surface. In aqueous solution without biomolecules, the amount of Cd in spot was within the range from 0 to 1000 ng. In the case of the mixture of QDs and MT, Cd amount was within the range from 0 to 500 ng per spot. The calibration curves of the aqueous solution of QDs were measured (not shown). The repeatability was not sufficient due to the poor tacking of particles on the polystyrene surface in the absence of biomolecule. In the presence of biomolecule — protein MT, the ability to capture on the polystyrene surface was higher in comparison with water solution of QDs and the measurement was sufficiently repeatable. The calibration curve and the maps with distribution for each amount of Cd (0–500 ng) on polystyrene surface are shown in Fig. 4. There is visible inhomogeneous distribution of Cd-QDs on the maps. Increased concentration at the edges of the spot is caused by drying effect and it can be a source of higher RSDs. The calibration curve includes the error bars from RSDs of Cd signal for 3 replicates, 3 spots respectively. The limits of detection determined for the LIBS measurements for QDs were calculated from $3\sigma/A$, where σ is the standard deviation of background signal and A is the slope of the calibration curve [32]. The limits of detection for CdTe QDs were 3 ng for CdS QDs, and 5 ng Cd per spot after injection of 5 μl of the mixture of QDs and MT. Further, we investigated the values of Cd signal after summarization including RSDs of the measurement with the increasing MT concentration within the range from 0 to 23 μmol l^{-1} (0–170 pg). The lowest RSD was achieved for the MT concentration of 2.3 μmol l^{-1}. For lower MT concentrations, the dried samples were peeled off from the polystyrene surface and created aggregate in the area of spot. Due to this, the effects for lower MT concentrations RSDs are higher. During our observation of other proteins, especially their interactions with QDs, it was found that higher protein concentration (in this case 23 μmol l^{-1} concentration) negatively influences not only the process of conjugation but also the analysis by LIBS itself.

3.3. Sandwich immunoassay

Further, we applied LIBS for the assessment of a metallothionein immunoassay [4,30]. Prior to the immunoassay, the detection steps were proven, especially fluorescence and LIBS detection of Cd distribution in spots with streptavidin-conjugated QDs and in spots with immobilized biotinylated antibodies and streptavidin-conjugated QDs. Firstly, the maps of Cd distribution in streptavidin-QDs conjugate spotted onto a polystyrene surface were measured. The distribution of Cd in the spots was consistent with the distribution of the fluorescence, with slight discrepancies caused by instable adsorption of QDs on polystyrene without the proteins (see above). However, the streptavidin-conjugated QDs were usable for further work.

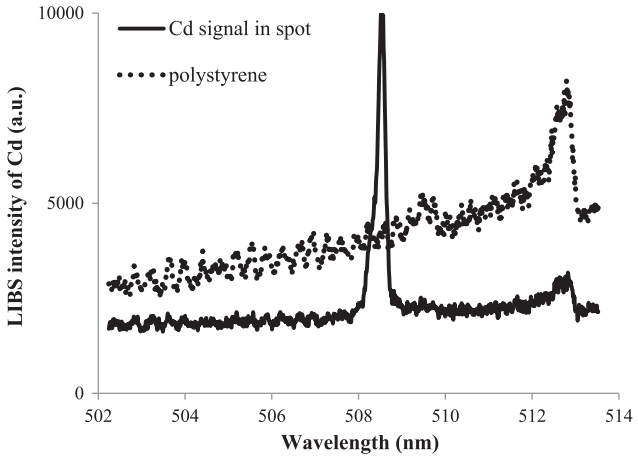

Fig. 3. Comparison of LIBS spectra: signal of Cd in spot containing 1000 ng of Cd and spectrum of polystyrene background.

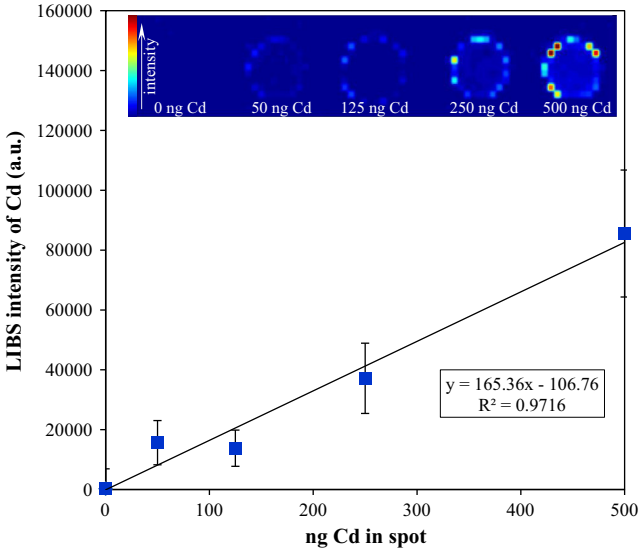

Fig. 4. The dependence of Cd signal measured by LIBS on Cd concentration (0–500 ng) in the spots on polystyrene surface and the distribution maps of Cd in the spots, the concentration of MT in the injected sample is 2.3 μmol l^{-1}.

In the next step, the binding of streptavidin-conjugated QDs with biotinylated antibodies was studied. It is known that streptavidin-biotin interaction is one of the strongest non-covalent interactions [33]. One of its practical application is (bio)molecules labeling in bioanalysis. The biotinylated and non-biotinylated antibodies were adsorbed onto a polystyrene surface and the streptavidin-conjugated QDs were added (Fig. 5A). After the interaction the solutions were removed, the surface was dried and both fluorescence and LIBS maps were obtained. From both measurements it was obvious that the signal intensity in spots with biotinylated antibody is higher, while at non-biotinylated antibody the fluorescence signal almost disappeared. This indicates that QDs were attached preferentially to biotinylated antibodies due to the streptavidin-biotin interaction.

To decrease blank Cd signal, the spots were washed with PBS. After washing, the sharp decrease of fluorescence was observed. However, the signal of Cd measured by LIBS was decreased only approximately to 50%. Except for the decrease of the blank Cd content, after washing the spots the broadening of the spots areas and formation of intensive spots borders occurred, probably due to the drying of spots.

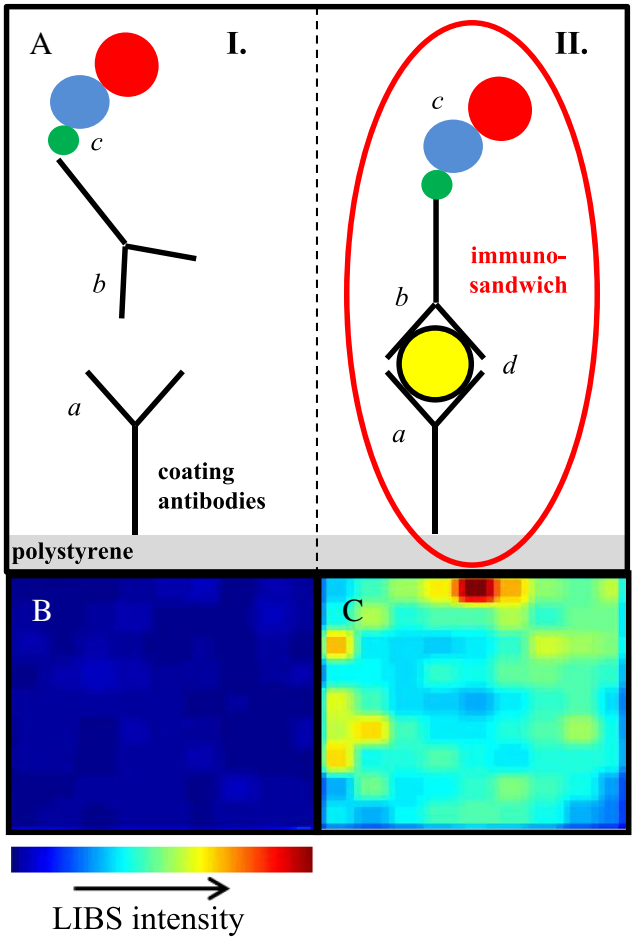

Fig. 5. (A) Scheme of immunosandwich preparation. I. (a) Antibodies are coated on the polystyrene. Further, biotinylated (green circle) anti-MT antibody (b) with (c) streptavidin-QDs (blue circle–red circle) unsuccessfully interacted with the coated antibody, because MT is missing. II. (a) Antibodies are coated on the polystyrene. Further, biotinylated (green circle) anti-MT antibody, (b) and (c) streptavidin-QDs (blue circle–red circle) successfully interacted with the coated antibody, because (d) MT is present (yellow circle). Cd distribution maps of spots (B) without MT and (C) with 70 pg MT. Onto a polystyrene surface of a microplate the coating anti-MT antibodies were deposited and samples with or without MT were added. Then biotinylated anti-MT antibodies and CdTe QDs-streptavidin were deposited. Each spot area was analyzed by LIBS on Cd emission line 508.58 nm. The maps made of reduced raster (9 × 9) points with spacing 500 μm show Cd occurrence in the presence of 70 pg of MT. (For interpretation of the references to color in this figure legend, the reader is referred to the web version of this article.)

After verification the usability of LIBS for detection of QDs-labeled antibodies, the sandwich immunoassay for MT was constructed. The unbound reagents were washed between the single steps with PBS. As it is obvious from Fig. 5B, the Cd content in spots with 70 pg of MT labeled with CdTe QDs (Fig. 5C) was significantly higher compared to spots without MT (Fig. 5B–C). To improve the spot assessment the ablation raster in the central area was decreased to 9 × 9 points with spacing 500 μm, which allowed us to eliminate the influence of the intensive spot border. When comparing the results obtained with results reported in [4], MT amount detected by LIBS is more than 10-times lower than the LOQ obtained by classical ELISA, e.g. 6.8 ng/ml or 680 pg per well [4]. From this point of view LIBS is suitable as a detection step in immunoassays employing QDs as a label.

4. Conclusion

Currently in immunoassay procedures the analyte determination based on QDs labeling uses their fluorescence or metal detection. Compared to these methods LIBS allows determination of not only the signal intensity, but also its spatial distribution. Although the QDs fluorescence is relatively stable compared to other labels, still the fluorescence quenching may occur and the immunoassay must be assessed immediately. LIBS offers also the possibility of dry immunoassay assessment and long-term storage of the processed samples before the assessment. Due to the immediate signal response, relatively simply instrumentation and possibility of automation LIBS offers promising and fast alternative to other detection techniques in immunoassay (especially if equipment with high repetition rate laser and detector will be used). It should be also noted that LIBS can serve not only for detection of quantum dots but also for nanoparticles which do not show any visible luminescence.

Acknowledgment

Financial support from the project CEITEC CZ.1.05/1.1.00/02.0068 is highly acknowledged.

References

[1] S. Krizkova, M. Ryvolova, J. Hrabeta, V. Adam, M. Stiborova, T. Eckschlager, R. Kizek, Metallothioneins and zinc in cancer diagnosis and therapy, Drug Metab. Rev. 44 (2012) 287–301.
[2] P. Babula, M. Masarik, V. Adam, T. Eckschlager, M. Stiborova, L. Trnkova, H. Skutkova, I. Provaznik, J. Hubalek, R. Kizek, Mammalians' metallothioneins and their properties and functions, Metallomics 4 (2012) 739–750.
[3] T. Eckschlager, V. Adam, J. Hrabeta, K. Figova, R. Kizek, Metallothioneins and cancer, Curr. Protein Pept. Sci. 10 (2009) 360–375.
[4] S. Krizkova, P. Blahova, J. Nakielna, I. Fabrik, V. Adam, T. Eckschlager, M. Beklova, Z. Svobodova, V. Horak, R. Kizek, Comparison of metallothionein detection by using Brdicka reaction and enzyme-linked immunosorbent assay employing chicken yolk antibodies, Electroanalysis 21 (2009) 2575–2583.
[5] V. Adam, I. Fabrik, T. Eckschlager, M. Stiborova, L. Trnkova, R. Kizek, Vertebrate metallothioneins as target molecules for analytical techniques, TrAC Trends Anal. Chem. 29 (2010) 409–418.
[6] H.W. Yu, J. Lee, S. Kim, G.H. Nguyen, I.S. Kim, Electrochemical immunoassay using quantum dot/antibody probe for identification of cyanobacterial hepatotoxin microcystin-LR, Anal. Bioanal. Chem. 394 (2009) 2173–2181.
[7] X.M. Pei, B. Zhang, J. Tang, B.Q. Liu, W.Q. Lai, D.P. Tang, Sandwich-type immunosensors and immunoassays exploiting nanostructure labels: a review, Anal. Chim. Acta. 758 (2013) 1–18.
[8] D.P. Tang, Y.L. Cui, G.A. Chen, Nanoparticle-based immunoassays in the biomedical field, Analyst 138 (2013) 981–990.
[9] O. Zitka, S. Krizkova, L. Krejcova, D. Hynek, J. Gumulec, M. Masarik, J. Sochor, V. Adam, J. Hubalek, L. Trnkova, R. Kizek, Microfluidic tool based on the antibody-modified paramagnetic particles for detection of 8-hydroxy-2′-deoxyguanosine in urine of prostate cancer patients, Electrophoresis 32 (2011) 3207–3220.
[10] D.P. Tang, B.L. Su, J. Tang, J.J. Ren, G.N. Chen, Nanoparticle-based sandwich electrochemical immunoassay for carbohydrate antigen 125 with signal enhancement using enzyme-coated nanometer-sized enzyme-doped silica beads, Anal. Chem. 82 (2010) 1527–1534.
[11] D.P. Tang, R. Yuan, Y.Q. Chal, Ultrasensitive electrochemical immunosensor for clinical immunoassay using thionine-doped magnetic gold nanospheres as labels and horseradish peroxidase as enhancer, Anal. Chem. 80 (2008) 1582–1588.

[12] V. Adam, J. Petrlova, J. Wang, T. Eckschlager, L. Trnkova, R. Kizek, Zeptomole electrochemical detection of metallothioneins, PLoS One 5 (2010) 11441–11448 (e11441).
[13] P. Sobrova, L. Vyslouzilova, O. Stepankova, M. Ryvolova, J. Anyz, L. Trnkova, V. Adam, J. Hubalek, R. Kizek, Tissue specific electrochemical fingerprinting, PLoS One 7 (2012) 1–12 (e49654).
[14] G.L. Damhorst, C.E. Smith, E.M. Salm, M.M. Sobieraj, H.K. Ni, H. Kong, R. Bashir, A liposome-based ion release impedance sensor for biological detection, Biomed. Microdevices 15 (2013) 895–905.
[15] C.F. Fronczek, D.J. You, J.Y. Yoon, Single-pipetting microfluidic assay device for rapid detection of *Salmonella* from poultry package, Biosens. Bioelectron. 40 (2013) 342–349.
[16] S. Lehmann, C. Delaby, J. Vialaret, J. Ducos, C. Hirtz, Current and future use of "dried blood spot" analyses in clinical chemistry, Clin. Chem. Lab. Med. 51 (2013) 1897–1909.
[17] J. Deglon, F. Versace, E. Lauer, C. Widmer, P. Mangin, A. Thomas, C. Staub, Rapid LC–MS/MS quantification of the major benzodiazepines and their metabolites on dried blood spots using a simple and cost-effective sample pretreatment, Bioanalysis 4 (2012) 1337–1350.
[18] R.M. Martin, R. Patel, E. Oken, J. Thompson, A. Zinovik, M.S. Kramer, K. Vilchuck, N. Bogdanovich, N. Sergeichick, Y. Foo, N. Gusina, Filter paper blood spot enzyme linked immunoassay for adiponectin and application in the evaluation of determinants of child insulin sensitivity, PLoS One 8 (2013) 1–10.
[19] F.J. Fortes, J.J. Laserna, The development of fieldable laser-induced breakdown spectrometer: no limits on the horizon, Spectrosc. Acta Part. B-At. Spectr. 65 (2010) 975–990.
[20] R.E. Russo, X.L. Mao, J.J. Gonzalez, V. Zorba, J. Yoo, Laser ablation in analytical chemistry, Anal. Chem. 85 (2013) 6162–6177.
[21] N.H. Bings, A. Bogaerts, J.A.C. Broekaert, Atomic spectroscopy: a review, Anal. Chem. 82 (2010) 4653–4681.
[22] J. Kaiser, K. Novotny, M.Z. Martin, A. Hrdlicka, R. Malina, M. Hartl, V. Adam, R. Kizek, Trace elemental analysis by laser-induced breakdown spectroscopy—biological applications, Surf. Sci. Rep. 67 (2012) 233–243.
[23] V. Motto-Ros, L. Sancey, X.C. Wang, Q.L. Ma, F. Lux, X.S. Bai, G. Panczer, O. Tillement, J. Yu, Mapping nanoparticles injected into a biological tissue using laser-induced breakdown spectroscopy, Spectrosc. Acta Pt. B-At. Spectr. 87 (2013) 168–174.
[24] M. Sovago, E.J. Buis, M. Sandtke, Nanoparticle detection in aqueous solutions using Raman and laser induced breakdown spectroscopy, Spectrosc. Acta Pt. B-At. Spectr. 87 (2013) 182–187.
[25] T. Borowik, M. Przybylo, K. Pala, J. Otlewski, M. Langner, Quantitative measurement of Au and Fe in ferromagnetic nanoparticles with laser induced breakdown spectroscopy using a polymer-based gel matrix, Spectrosc. Acta Part B-At. Spectr. 66 (2011) 726–732.
[26] A. De Giacomo, R. Gaudiuso, C. Koral, M. Dell'Aglio, O. De Pascale, Nanoparticle-enhanced laser-induced breakdown spectroscopy of metallic samples, Anal. Chem. 85 (2013) 10180–10187.
[27] D. Prochazka, L. Ballova, K. Novotny, J. Novotny, R. Malina, P. Babula, V. Adam, R. Kizek, K. Procházková, K. J., Optimization of laser-induced breakdown spectroscopy (LIBS) for determination of quantum dots (Qds) in liquid solutions, World Acad. Sci. Eng. Technol. 6 (2012) 1815–1818.
[28] H. Li, W.Y. Shih, W.H. Shih, Synthesis and characterization of aqueous carboxyl-capped CdS quantum dots for bioapplications, Ind. Eng. Chem. Res. 46 (2007) 2013–2019.
[29] S. Skalickova, O. Zitka, L. Nejdl, S. Krizkova, J. Sochor, L. Janu, M. Ryvolova, D. Hynek, J. Zidkova, V. Zidek, V. Adam, R. Kizek, Study of interaction between metallothionein and CdTe quantum dots, Chromatographia 76 (2013) 345–353.
[30] S. Krizkova, V. Adam, T. Eckschlager, R. Kizek, Using of chicken antibodies for metallothionein detection in human blood serum and cadmium-treated tumour cell lines after dot- and electroblotting, Electrophoresis 30 (2009) 3726–3735.
[31] R.W.B. Pearse, A.G. Gaydon, The Identification of Molecular Spectra, 4th ed. Chapman and Hall, London and New York, 1976.
[32] G.L. Long, J.D. Winefordner, Limit of detection, Anal. Chem. 55 (1983) A712–A724.
[33] C.E. Chivers, A.L. Koner, E.D. Lowe, M. Howarth, How the biotin-streptavidin interaction was made even stronger: investigation via crystallography and a chimaeric tetramer, Biochem. J. 435 (2011) 55–63.